Neovascularization in the outer membrane of chronic subdural hematomas from the dural border cell layer of the dura mater

Hyun Kim
Seoul National University
Yoori Choi (yns086@snu.ac.kr)
Seoul National University Hospital https://orcid.org/0000-0002-4634-5974
Youngsun Lee
Seoul National University
Jae-Kyung Won
Seoul National University Hospital
Sung Ho Lee
Seoul National University Hospital
Minseok Suh
Seoul National University Hospital
Dong Soo Lee
Seoul National University
Hyun-Seung Kang
Seoul National University Hospital
Won-Sang Cho
Seoul National University Hospital
Gi Jeong Cheon
Seoul National University Hospital

Research Article

Keywords: Chronic subdural hematoma, Dural border cell layer, Outer membrane, Neovascularization, Lymphangiogenesis

Posted Date: July 1st, 2022

DOI: https://doi.org/10.21203/rs.3.rs-1732837/v1

Abstract

Chronic subdural hematomas (cSDHs) are generally known to result from traumatic tears of bridging veins. However, the causes of repeat spontaneous cSDHs are still unclear. We investigated the changes in vasculature in the human dura mater and outer membrane (OM) of cSDHs to elucidate the cause of their spontaneous repetition. The dura mater was obtained from a normal control participant and a patient with repeat spontaneous cSDHs. The pathological samples from the patient included the dura mater and OM tightly adhered to the inner dura. The samples were analyzed with a particular focus on blood and lymphatic vessels by immunohistochemistry, 3-dimensional imaging using a transparent tissue clearing technique, and electron microscopy. The dural border cell (DBC) layer of the dura mater and OM were histologically indistinguishable. There were 5.9 times more blood vessels per unit volume of tissue in the DBC layer and OM in the patient than in the normal control. The DBC layer and OM contained pathological sinusoidal capillaries not observed in the normal tissue; these capillaries were connected to the middle meningeal arteries via penetrating arteries. In addition, marked lymphangiogenesis in the periosteal and meningeal layers was observed in the patient with cSDHs. Neovascularization in the OM seemed to originate from the DBC layer; this is a potential cause of repeat spontaneous cSDHs. Embolization of the meningeal arteries to interrupt the blood supply to pathological capillaries via penetrating arteries may be an effective treatment option.

Introduction

A chronic subdural hematoma (cSDH) is characterized by blood accumulation between the dura and arachnoid mater that develops over 3 weeks or more [1]. The annual incidence of cSDHs is approximately 17.6 per 100,000 individuals, and cSDHs increase significantly in the population aged 80 years and older (52.1 for 70–79-year-olds versus 130.3 for 80–89-year-olds per 100,000/year) [2,3]. Approximately 50 ~ 80% of patients with cSDHs have a history of head trauma and the use of antithrombotic agents [1,4,5]. SDHs are commonly caused by tears in bridging veins and rarely by ruptures of arterial twigs traversing the subdural space [6,7]. Hematomas can regress spontaneously [8] or with the aid of medications such as steroids [8], tranexamic acid [9], angiotensin-converting enzyme inhibitors [10] and platelet-activating factor receptor antagonists [11]. However, due to the mass effect of cSDHs, symptomatic patients must be treated with surgical interventions such as burr hole trephination and craniotomy [12].

The recurrence rate of cSDHs has been reported to be 2 ~ 37%, even after surgical management [13]. Although cSDHs usually recur due to known causes such as trauma, drugs and clinical diseases, their spontaneous repetition is expected to be due to other causes. Previous studies have proposed several hypotheses for repeat spontaneous occurrence of cSDHs: the formation of a leaky vascularized outer membrane (OM) [1,14,15], clotting cascade dysfunction [16], the transfer of cerebrospinal fluid into the hematoma by the osmotic gradient [1,4,17], and local hyperfibrinolysis [1,4,17].

Recently, embolization of the middle meningeal arteries (MMAs) supplying the dura mater with glue or particles was reported to have a significantly lower recurrence rate and a higher cure rate than conventional management [18–20]. These clinical results are considered strong evidence of the direct relationship between MMAs and repeat spontaneous cSDHs [18–20]. Nevertheless, translational studies supporting this hypothesis are still lacking [21]. We aimed to elucidate the pathophysiology of repeat spontaneous cSDHs through the histopathological comparison of the dura mater and membrane enveloping cSDHs between a normal control participant and a patient with repeat spontaneous cSDHs.

Materials And Methods

Sampling of normal and pathological dura mater

Human dura mater samples were acquired under the approval of the institutional review board. The normal dura mater was acquired from a patient undergoing surgical clipping of an unruptured intracranial aneurysm who had no history of intracranial disease (normal control). A large dura mater with cSDHs was harvested from a patient who underwent left-sided frontotemporal craniotomy, clipping of an unruptured aneurysm in the anterior communicating artery and evacuation of the multilayered cSDHs (pathological case) (Fig. 1a). As blood accumulates in the subdural space, a new membrane forms that envelops the SDHs. Based on previous studies [1,14,15,17], the newly formed membrane between the dura mater and hematoma was defined as the OM, and the membrane between the hematoma and arachnoid mater was defined as the inner membrane in this study. Intraoperatively, the cSDHs were found to be covered with outer and inner membranes and separated with a few intervening membranes, in which the slightly thickened OM was attached to the inner surface of the dura mater; meanwhile, the thinner inner membrane was less firmly attached to the arachnoid mater. Intramembranous contents included dark brownish fluid and a solid, old clot. When the OM was peeled from the inner surface of the dura mater, fine blood oozing from the inner dural surface was observed in that area. However, there was no such microscopic finding of bleeding upon removing the inner membrane from the arachnoid mater. A large dura mater attached to the OM of the cSDHs was resected, and the dural defect was replaced with artificial dural materials in the patient (Fig. 1b).

Tissue clearing

Dural samples were fixed in 10% formalin after harvest and stored at 4 °C for at least 24 hours. The samples were cut into smaller pieces and put in acrylamide solution for hydrogel embedding. After an overnight incubation at 4 °C, the bottle containing acrylamide solution was filled with nitrogen gas, and the samples were incubated at 37 °C for 5 hours. Lipids were cleared from the polymerized tissues through electrophoresis. To increase tissue permeability, the samples were incubated in DeepLabel™ solution A (Logos Biosystem, #C33002) for 3 days. For immunostaining, the samples were incubated at 37 °C with primary antibodies against the following proteins in DeepLabel™ solution B (Logos Biosystem, #C33003): laminin (Sigma Aldrich, #L9393), α-smooth muscle actin (αSMA; Abcam, #ab7817), and podoplanin (PDPN; Abcam, #ab77854; Santa Cruz Biotechnology, #sc-376695). After 7 days of

incubation, the dural samples were washed with phosphate-buffered saline (PBS) and incubated for 5 days with the following secondary antibodies: Alexa Flour™ 488 goat anti-mouse IgG (Invitrogen, #A11001), Alexa Flour™ 594 goat anti-mouse IgG (Invitrogen, #A11005), Alexa Flour™ 488 goat anti-rabbit IgG (Invitrogen, #A11008), Alexa Flour™ 488 chicken anti-goat IgG (Invitrogen, #A21467), Alexa Flour™ 647 chicken anti-rabbit IgG (Invitrogen, #A21443), and Alexa Flour™ 555 donkey anti-rabbit IgG (Invitrogen, #A31572). Washed samples were mounted overnight in X-CLARITY™ mounting solution (Logos Biosystem, #C13101). Images of the stained samples were obtained using a Leica SP8 confocal microscope.

Immunohistochemistry

Selected regions of the dural samples were embedded in paraffin and sectioned at 4 μm. These sectioned samples were deparaffinized in xylene and rehydrated serially in 100–70% ethanol solutions. After antigen retrieval using citric acid and trisodium citrate for 50 minutes, the permeability of the samples was increased using 0.5% Triton X-100 in PBS, and nonspecific antigens were blocked using 5% bovine serum albumin in PBS. Then, primary antibodies were added to the sectioned samples overnight at 4 °C. The primary antibodies used for targeting antigens were the same as those used in CLARITY. After overnight incubation, the slides were washed and incubated for 1 hour with the same secondary antibodies used in CLARITY. The samples were washed again and mounted using VECTASHEILD® mounting solution (Vector Laboratories, #H-1000). Similar to the CLARITY procedure, a Leica SP8 confocal microscope was used to capture images of stained samples.

Volume measurement of vessels

To measure the volume of whole tissues and stained vasculature, IMARIS (Oxford instrument) was used. After reconstruction of the 3-dimensional (3D) vascular architecture, the surface analysis technique in IMARIS extracted quantification values of vasculature in the tissue. The obtained values represent the volume (μm^3) of immunofluorescence-positive vessels per unit volume (μm^3) of tissue. To estimate vascular formation, vascular volume density was measured in 3 pieces of normal dura mater and 3 pieces of pathological dura mater with the OM of cSDHs. Additionally, another 3 pieces from the normal control and pathological dural samples were used for measuring artery volume density.

Transmission electron microscopy (TEM)

TEM (JEOL, JEM-1400) images were taken at our institution. The dural samples were fixed in 10% formalin and washed in PBS overnight. Then, the samples were washed in Sorensen's phosphate buffer and fixed in 2% osmium tetroxide. After dehydration in alcohol, propylene was added, and the samples were embedded in Spurr's embedding media. Ultrathin sectioned samples were mounted on copper grids and stained with uranyl acetate and lead citrate.

Statistical analysis

Data were statistically analyzed with Prism and Real Statistics/Excel software. Values are reported as the average ± standard deviation (SD). One-way ANOVA with post hoc Tukey's test was used for multiple comparisons. An unpaired t-test was used to compare the number of blood vessels, lymphatic sprouts and loops and the vascular volume density. Significant differences were indicated by $p < 0.05$ (*) and $p < 0.005$ (**).

Results

Structural changes in dural layers

After H&E staining of the normal control sample, the dura mater was divided into 3 layers separated from the superficial layer: the periosteal, meningeal and dural border cell (DBC) layers. MMAs were present in the periosteal layer. The meningeal layer had less collagen and denser cells than the periosteal layer. The DBC layer, the deepest layer, was the thinnest and contained less fibrous connective tissues than the other layers (Fig. 1c, d). The structures of the periosteal and meningeal layers in the dura mater were not different in the patient with cSDHs and the normal control. Between the meningeal dural layer and hematoma, however, there was a loose and thick layer where the DBC layer and OM of the cSDHs were located. This layer contained loose connective tissues, numerous vessels and erythrocytes (Fig. 1c, d). Although the DBC layer and OM could be easily separated mechanically, they appeared histologically indistinguishable.

Neovascularization in the DBC layer of the dura mater and OM of cSDHs

To observe the vascular structures, we stained the membranes with laminin, a basal membrane marker of vascular structures such as arteries, capillaries, veins and lymphatic vessels, and αSMA, an arterial marker for mural cells and pericytes. The average number of laminin-positive vessels per area (mm^2) was 20.77 ± 9.86 in the DBC layer of the normal dura mater and 78.96 ± 7.49 in the DBC layer and OM in the dura mater from the patient with cSDHs, which was an approximately 3.8-fold difference (Fig. 2a, b). To analyze the vasculature pattern, 3D laminin-positive vessels were observed in the transparent dura mater (Fig. 2c, d). The percentage of vasculature volume density (μm^3) was 5.9 times higher in the patient with cSDHs than in the normal control (Fig. 2e).

Pathological sinusoidal capillaries in the DBC layer of the dura mater and OM of cSDHs

To understand the characteristics of the newly formed vessels, we observed the structural characteristics of the endothelial cells in vessels of the DBC layer in the normal control and in vessels of the DBC layer and OM in the patient with cSDHs using TEM. In the DBC layer of the normal control and the DBC layer and OM in the patient, continuous capillaries were present (Fig. 3a). This type of capillary contains endothelial cells connected by tight junctions. Interestingly, fenestrated and sinusoidal capillaries were observed in only the DBC layer and OM in the patient with cSDHs. The endothelial cells in the fenestrated capillaries had pores with diaphragms, and sinusoidal capillaries showed gaps between endothelial cells (Fig. 3b). In addition, capillaries (defined as 5~10 μm in diameter [22]) with gaps between αSMA-stained

cells were observed in the DBC layer and OM of cSDHs. The αSMAs in the DBC layer and OM were thinner in the patient than in the normal control (Supplementary Fig. 1, online resource).

Penetrating arteries connecting MMAs in the periosteal layer and capillaries in the DBC layer and OM of cSDHs

To confirm the blood supply to the newly formed vessels in the DBC layer and OM of the cSDHs, arteries throughout the dura mater were constructed in 3D. Dural arteries in the transparent tissue samples were stained with laminin and αSMA antibodies, and the MMAs in the periosteal layer were observed to branch to the DBC layer in the normal control and to the DBC layer and OM in the patient with cSDHs. The diameters of MMAs in the periosteal dural layer and MMA-derived penetrating arteries ranged from 100 to 600 μm and from 20 to 50 μm, respectively (Supplementary Table 1, online resource). Penetrating arteries passed the meningeal dural layer and finally connected to the capillaries distributed in the DBC layer of the normal control and the DBC layer and OM of the patient with cSDHs (Fig. 4a). There were no differences in the number or diameter of MMAs and penetrating arteries between the normal control and patient with cSDHs (Supplementary Table 1, online resource). To confirm the formation of arterioles and capillaries connected to penetrating arteries, the volume of αSMA-positive vessels in a unit volume (μm^3) was measured. The arterial volume density in the DBC layer and OM of the cSDHs was 5.4 times higher than that in the normal DBC layer (Fig. 4b, videos 1, 2). The diameter of blood vessels in the DBC layer and OM of cSDHs was not different compared with the normal control, so the increase in vascular volume suggested an increase in the number of vessels (Supplementary Table 1, online resource).

Lymphangiogenesis in the periosteal to meningeal dural layers

To identify the induction of lymphangiogenesis during laminin-positive angiogenesis, PDPN antibodies were used for immunostaining of lymphatic endothelial cells. Interestingly, sprouts and loops of lymphatic vessels, morphological characteristics of newly formed lymphatic vessels, were observed in both the normal control and pathological dura mater samples (Fig. 5a). Newly formed lymphatic vessels were highly developed, especially around large vessels in the periosteal layer from the patient with cSDHs (Fig. 5b); however, lymphatics in the DBC layer and OM could not be observed due to technical limitations. The numbers of sprouts and loops were counted to obtain the average per volume (μm^3). The average number of sprouts per volume in the normal control and patient dura mater samples was 0.25±0.49 and 6.64±8.3, respectively; the patient with cSDHs had 26.9 times more sprouts than the normal control. The average number of loops per volume (μm^3) in the normal control and patient was 0.069±0.08 and 4.03±3.04, respectively, suggesting that the patient had 58.8 times more loops than the normal control (Fig. 5c).

Discussion

To clarify the pathophysiology of repeat spontaneous cSDHs, we investigated tissue samples of the dura mater and cSDH membranes from a patient with repeat spontaneous cSDHs and a normal control. A

thick DBC layer and OM of the cSDHs that were not histologically distinguishable were observed in the patient with cSDHs. Extensive laminin-positive neovascularization in the DBC layer and OM in the patient resulted in a 5.9-fold higher vasculature volume density than in the normal DBC layer. Fragile pathological sinusoidal capillaries that were not detected in the normal dura mater were observed in the DBC layer and OM. The vasculature was widely distributed in DBC layer, and the OM was connected to the MMAs in the periosteal layer through the penetrating arteries. In addition, the formation of lymphatic vessels in the periosteal and meningeal layers in the patient with cSDHs was increased compared to that in the normal control. Based on these findings, it can be postulated that an incomplete but abundantly neovascularized OM of cSDHs forms from the DBC layer of the dura mater, and repeat spontaneous bleeding occurs from the fragile pathological capillaries in the OM of cSDHs that connect to MMAs via penetrating arteries.

According to previous reports [1,14,15,17], the histological characteristics of cSDHs are as follows: 1) blood collects between the DBC layer of the dura mater and arachnoid mater; 2) outer and inner membranes (neomembranes) of cSDHs form with fibroblasts and collagen fibers; and 3) extensive neovascularization with sinusoidal capillaries occurs in the DBC dural layer and OM of cSDHs. The blood components that accumulate between the dura and arachnoid mater stimulate the recruitment of inflammatory cells to repair the damaged DBC layer by forming granulation tissues. Type 1 (PICP) and type 3 (PIIINP) procollagens, which are abundant in SDHs, also induce the proliferation of fibrous connective tissues in the DBC layer [1]. This process is similar to that during wound healing and is known as neomembrane formation [1,17]. It has been reported that the inner membrane is generally not associated with neovascularization, and blood vessels in the inner membrane disappear as cSDHs mature [18]. Meanwhile, neovascularization develops in the OM of cSDHs, and the neovascularized OM has been suspected to evoke the growth of cSDHs [18]. Additionally, in this study, we observed a histologically indistinguishable DBC layer of the dura mater and OM of cSDHs. Accordingly, we considered that the neovascularized OM forms from the DBC layer in the dura mater facing cSDHs.

Neovascularization in the OM of cSDHs is thought to be a result of the hematoma. As blood accumulates in the subdural space, inflammatory cells, including neutrophils, lymphocytes, macrophages and erythrocytes, migrate and release cytokines and angiogenetic factors around the hematoma and adjacent dural layer [16,17]. Usually, the presence of proinflammatory cytokines such as IL-2, IL-5, IL-6, IL-7 and IL-8 increases to a greater extent than that of anti-inflammatory cytokines such as IL-10 and IL-13 [16]. The concentration of VEGF, a characteristic angiogenic factor, is much higher in SDHs than in peripheral blood. The level of angiopoietin-2, which normally promotes cell death and disrupts vessels, increases more in the OM than in the brain parenchyma, promoting neovascularization in the OM as it cooperates with VEGF [23]. In addition, the concentration of VEGF-2, which is known to play a critical role in the regeneration of meningeal vessels after head injury, increases substantially [24]. Based on this background evidence, a phase II randomized proof-of-concept clinical trial with atorvastatin for immunoregulation and dexamethasone for vascular repair was conducted in patients with cSDHs [25]. The results showed that atorvastatin combined with low-dose dexamethasone reduced hematoma and improved neurological function. This finding suggests that inflammation and neovascularization may be closely related to

repeat spontaneous bleeding, and the modulation of associated factors is a potential therapeutic target for the resolution of cSDHs.

In general, there are three types of capillaries, continuous, fenestrated and sinusoidal capillaries that can be distinguished by endothelial cell structures. Continuous capillaries have tight junctions between endothelial cells, and fenestrated capillaries have pores with diaphragms between endothelial cells. Continuous and fenestrated capillaries are known to exist in the normal dura mater; however, only continuous capillaries were identified in this study. Sinusoidal capillaries are mainly found in the liver, spleen, bone marrow, and brain circumventricular organs but not in the dura mater [22]. Thus, the observation of sinusoidal capillaries in the DBC dural layer and OM indicates pathological changes in cSDHs [15]. In this study, pathological sinusoidal capillaries were observed in the DBC layer of the dura mater and OM of cSDHs but not in the normal control. Sinusoidal capillaries (or macrocapillaries) have been considered fragile and leaky compared with other types of capillaries because of certain characteristics, such as thin or absent basement membranes, a lack of smooth muscle cells and pericytes, and gaps [14,17]. Therefore, these capillaries have been considered the main cause of repeat bleeding [1,14,15]. The osmotic-oncotic pressure hypothesis involving the transport of CSF into the encapsuled hematoma has been suggested as another cause of repeat spontaneous cSDHs [26]. However, this theory has now been discarded because studies failed to demonstrate differences in osmotic-oncotic pressure among hematomas, plasma and cerebrospinal fluid [4]. The clotting cascade dysfunction hypothesis posits that the subdural blood clot liquefies and causes persistent bleeding [27], and the local hyperfibrinolysis hypothesis involves excessive fibrinolytic activity due to a pre-existing latent coagulation disorder. However, these hypotheses cannot explain most cases of repeat spontaneous cSDHs [28].

For the past two decades, since the first case report of cSDHs refractory to several surgical procedures in 2000, embolization of MMAs with glue and particles has shown potential as an alternative to conventional surgery [18,21,29]. A recent meta-analysis showed that the recurrence rate after MMA embolization was 2.4% for recurrent cSDHs and 4.1% for primary cSDHs compared to the usual postoperative recurrence rate of 10–20%, confirming the excellent inhibitory effect of MMA embolization on cSDHs [29,30]. The newly formed capillaries located in the DBC layer of the dura mater and OM of cSDHs were found to be connected to MMAs in the periosteal dural layer via penetrating arteries in this study. Based on such histological findings, it is speculated that MMA embolization can block the blood supply to sinusoidal capillaries (Fig. 6). In brief, a microcatheter is inserted into MMAs ipsilateral to cSDHs via the external carotid artery, and then, glue or particles are injected into the MMAs to interrupt the blood supply to the targeted dura mater [19].

In the pathological dura mater facing the cSDHs, greater increases in lymphangiogenesis and blood vessels were observed compared to the normal control (Fig. 5). The morphological changes such as sprouting and loop formation of the lymphatics observed in this study are generally seen during angiogenesis and lymphatic vessel regeneration after traumatic brain injury [31,32]. The meningeal lymphatic system is known to be involved in passing immune cells and draining waste from the brain to

the deep cervical lymph nodes [33]. In addition, an animal study showed that hematomas drained out of the subdural space through the meningeal lymphatic vessels and lymphatic dysfunction caused by meningeal lymphatic ligation led to the attenuation of SDH resorption [34]. Therefore, it may be a general concept that blood components are resolved throughout the meningeal veins and lymphatics once SDHs accumulate. Meanwhile, if spontaneous bleeding from the neovascularized OM of cSDHs occurs repeatedly, the accumulation of cSDHs could surpass the resorption capacity of the meningeal veins and lymphatics, ultimately resulting in clinical symptoms and signs. In such a repetitive situation, symptomatic cSDHs can be treated by craniotomy followed by removal of the neovascularized dura mater and OM or MMA embolization rather than by simple burr hole trephination.

In summary, neovascularization with pathological sinusoidal capillaries were observed in the DBC dural layer and OM of cSDHs. The pathological capillaries were connected to MMAs via penetrating arteries. Based on these findings in this study, the neovascularized OM of cSDHs may form from the DBC layer of the dura mater, and repeat spontaneous cSDHs may originate from the neovascularized OM. Interruption of the blood supply to the neovascularized OM of cSDHs could lead to resolution via the meningeal veins and lymphatics. Thus, MMA embolization appears to be very promising as a less invasive treatment for patients with repeat spontaneous cSDHs.

Abbreviations

cSDH
chronic subdural hematoma
OM
outer membrane
DBC
dural border cell
MMA
middle meningeal artery
αSMA
α-smooth muscle actin
PDPN
podoplanin
PBS
phosphate buffered saline
TEM
transmission electron microscopy
SD
standard deviation

Declarations

Ethical Approval and Consent to participate

Human samples were acquired under the approval of the Seoul National University Hospital institutional review board.

Availability of data and materials

All data generated or analyzed during this study are included in this published article (and its supplementary information files).

Competing interests

The authors declare no competing financial interests.

Funding

This research was supported by the National Research Foundation of Korea Grant funded by the Korea Government (No. NRF-2017M3C7A1048079, NRF-2020R1A2C2101069, NRF-2020M2D9A1093988) and also supported by a grant of the Korea Medical Device Development Fund (the Ministry of Science and ICT, the Ministry of Trade, Industry and Energy, the Ministry of Health & Welfare, the Ministry of Food and Drug Safety) (KMDF_PR_20200901_0137). And this work was supported by the New Faculty Startup Fund from Seoul National University (800-20200264)

Author contributions

W.S.C., Y.C., G.J.C. designed the study. S.H.L isolated human dura samples. H.K., Y.L. performed experiments and D.S.L., M.S., H.S.K. performed data analyses. J.K.W. contributed to confirming the pathology. K.H., Y.C., and W.S.C wrote the paper. All authors read and approved the final manuscript.

Acknowledgments

The Biospecimens and data used in this study were provided by the Biobank of Seoul National University Hospital, a member of Korea Biobank Network (KBN4_A03)

References

1. Sahyouni R, Goshtasbi K, Mahmoodi A, Tran DK, Chen JW (2017) Chronic Subdural Hematoma: A Perspective on Subdural Membranes and Dementia. World Neurosurg Dec 108:954–958. doi:10.1016/j.wneu.2017.09.063
2. Rauhala M, Luoto TM, Huhtala H et al (2019) The incidence of chronic subdural hematomas from 1990 to 2015 in a defined Finnish population. J Neurosurg Mar 22(4):1147–1157. doi:10.3171/2018.12.JNS183035

3. Yang W, Huang J (2017) Chronic Subdural Hematoma: Epidemiology and Natural History. Neurosurg Clin N Am Apr 28(2):205–210. doi:10.1016/j.nec.2016.11.002
4. Chen JC, Levy ML (2000) Causes, epidemiology, and risk factors of chronic subdural hematoma. Neurosurg Clin N Am Jul 11(3):399–406
5. Sim YW, Min KS, Lee MS, Kim YG, Kim DH (2012) Recent changes in risk factors of chronic subdural hematoma. J Korean Neurosurg Soc Sep 52(3):234–239. doi:10.3340/jkns.2012.52.3.234
6. Cho WS, Batchuluun B, Lee SJ, Kang HS, Kim JE (2011) Recurrent subdural hematoma from a pseudoaneurysm at the cortical branch of the middle cerebral artery after mild head injury: case report. Neurol Med Chir (Tokyo) 51(3):217–221. doi:10.2176/nmc.51.217
7. Rambaud C (2015) Bridging veins and autopsy findings in abusive head trauma. Pediatr Radiol Jul 45(8):1126–1131. doi:10.1007/s00247-015-3285-0
8. Parlato C, Guarracino A, Moraci A (2000) Spontaneous resolution of chronic subdural hematoma. *Surg Neurol*. ;53(4):312-5; discussion 315-7. doi:10.1016/s0090-3019(00)00200-7
9. Kageyama H, Toyooka T, Tsuzuki N, Oka K (2013) Nonsurgical treatment of chronic subdural hematoma with tranexamic acid. J Neurosurg Aug 119(2):332–337. doi:10.3171/2013.3.JNS122162
10. Weigel R, Hohenstein A, Schlickum L, Weiss C, Schilling L (2007) Angiotensin converting enzyme inhibition for arterial hypertension reduces the risk of recurrence in patients with chronic subdural hematoma possibly by an antiangiogenic mechanism. Neurosurg Oct 61(4):788–792 discussion 792-3. doi:10.1227/01.NEU.0000298907.56012.E8
11. Hirashima Y, Kurimoto M, Nagai S, Hori E, Origasa H, Endo S (2005) Effect of platelet-activating factor receptor antagonist, etizolam, on resolution of chronic subdural hematoma–a prospective study to investigate use as conservative therapy. Neurol Med Chir (Tokyo) Dec 45(12):621–626 discussion 626. doi:10.2176/nmc.45.621
12. Mehta V, Harward SC, Sankey EW, Nayar G, Codd PJ (2018) Evidence based diagnosis and management of chronic subdural hematoma: A review of the literature. J Clin Neurosci Apr 50:7–15. doi:10.1016/j.jocn.2018.01.050
13. Ohba S, Kinoshita Y, Nakagawa T, Murakami H (2013) The risk factors for recurrence of chronic subdural hematoma. Neurosurg Rev Jan 36(1):145–149 discussion 149 – 50. doi:10.1007/s10143-012-0396-z
14. Shim YS, Park CO, Hyun DK, Park HC, Yoon SH (2007) What are the causative factors for a slow, progressive enlargement of a chronic subdural hematoma? Yonsei Med J Apr 30(2):210–217. doi:10.3349/ymj.2007.48.2.210
15. Yamashima T, Yamamoto S, Friede RL (1983) The role of endothelial gap junctions in the enlargement of chronic subdural hematomas. J Neurosurg Aug 59(2):298–303. doi:10.3171/jns.1983.59.2.0298
16. Stanisic M, Aasen AO, Pripp AH et al (2012) Local and systemic pro-inflammatory and anti-inflammatory cytokine patterns in patients with chronic subdural hematoma: a prospective study. Inflamm Res Aug 61(8):845–852. doi:10.1007/s00011-012-0476-0

17. Edlmann E, Giorgi-Coll S, Whitfield PC, Carpenter KLH, Hutchinson PJ (2017) Pathophysiology of chronic subdural haematoma: inflammation, angiogenesis and implications for pharmacotherapy. J Neuroinflammation May 30(1):108. doi:10.1186/s12974-017-0881-y
18. Ban SP, Hwang G, Byoun HS et al (2018) Middle Meningeal Artery Embolization for Chronic Subdural Hematoma. Radiol Mar 286(3):992–999. doi:10.1148/radiol.2017170053
19. Link TW, Boddu S, Paine SM, Kamel H, Knopman J (2019) Middle Meningeal Artery Embolization for Chronic Subdural Hematoma: A Series of 60 Cases. Neurosurg Dec 1(6):801–807. doi:10.1093/neuros/nyy521
20. Srivatsan A, Mohanty A, Nascimento FA et al (2019) Middle Meningeal Artery Embolization for Chronic Subdural Hematoma: Meta-Analysis and Systematic Review. World Neurosurg Feb 122:613–619. doi:10.1016/j.wneu.2018.11.167
21. Shapiro M, Walker M, Carroll KT et al (2021) Neuroanatomy of cranial dural vessels: implications for subdural hematoma embolization. J Neurointerv Surg Feb 25. doi:10.1136/neurintsurg-2020-016798
22. Augustin HG, Koh GY (2017) Organotypic vasculature: From descriptive heterogeneity to functional pathophysiology. Sci Aug 25(6353). doi:10.1126/science.aal2379
23. Weigel R, Schilling L, Schmiedek P (2001) Specific pattern of growth factor distribution in chronic subdural hematoma (CSH): evidence for an angiogenic disease. Acta Neurochir (Wien) Aug 143(8):811–818 discussion 819. doi:10.1007/s007010170035
24. Koh BI, Lee HJ, Kwak PA et al (2020) VEGFR2 signaling drives meningeal vascular regeneration upon head injury. Nat Commun Jul 31(1):3866. doi:10.1038/s41467-020-17545-2
25. Wang D, Gao C, Xu X et al Treatment of chronic subdural hematoma with atorvastatin combined with low-dose dexamethasone: phase II randomized proof-of-concept clinical trial.J Neurosurg. Jan31 2020:1–9. doi: 10.3171/2019.11.JNS192020
26. GARDNER WJ. TRAUMATIC SUBDURAL HEMATOMA: WITH PARTICULAR REFERENCE TO THE LATENT INTERVAL (1932) Archives of Neurology & Psychiatry 27(4):847–858. doi:10.1001/archneurpsyc.1932.02230160088009
27. Kawakami Y, Chikama M, Tamiya T, Shimamura Y (1989) Coagulation and fibrinolysis in chronic subdural hematoma. Neurosurg Jul 25(1):25–29. doi:10.1097/00006123-198907000-00005
28. Ito H, Yamamoto S, Komai T, Mizukoshi H (1976) Role of local hyperfibrinolysis in the etiology of chronic subdural hematoma. J Neurosurg Jul 45(1):26–31. doi:10.3171/jns.1976.45.1.0026
29. Fiorella D, Arthur AS (2019) Middle meningeal artery embolization for the management of chronic subdural hematoma. J Neurointerv Surg Sep 11(9):912–915. doi:10.1136/neurintsurg-2019-014730
30. Haldrup M, Ketharanathan B, Debrabant B et al (2020) Embolization of the middle meningeal artery in patients with chronic subdural hematoma-a systematic review and meta-analysis. Acta Neurochir (Wien) Apr 162(4):777–784. doi:10.1007/s00701-020-04266-0
31. Blanco R, Gerhardt H (2013) VEGF and Notch in tip and stalk cell selection. Cold Spring Harb Perspect Med Jan 1(1):a006569. doi:10.1101/cshperspect.a006569

32. Bolte AC, Dutta AB, Hurt ME et al (2020) Meningeal lymphatic dysfunction exacerbates traumatic brain injury pathogenesis. Nat Commun Sep 10(1):4524. doi:10.1038/s41467-020-18113-4
33. Louveau A, Smirnov I, Keyes TJ et al (2015) Structural and functional features of central nervous system lymphatic vessels. Nat Jul 16(7560):337–341. doi:10.1038/nature14432
34. Liu X, Gao C, Yuan J et al (2020) Subdural haematomas drain into the extracranial lymphatic system through the meningeal lymphatic vessels. Acta Neuropathol Commun Feb 14(1):16. doi:10.1186/s40478-020-0888-y

Figures

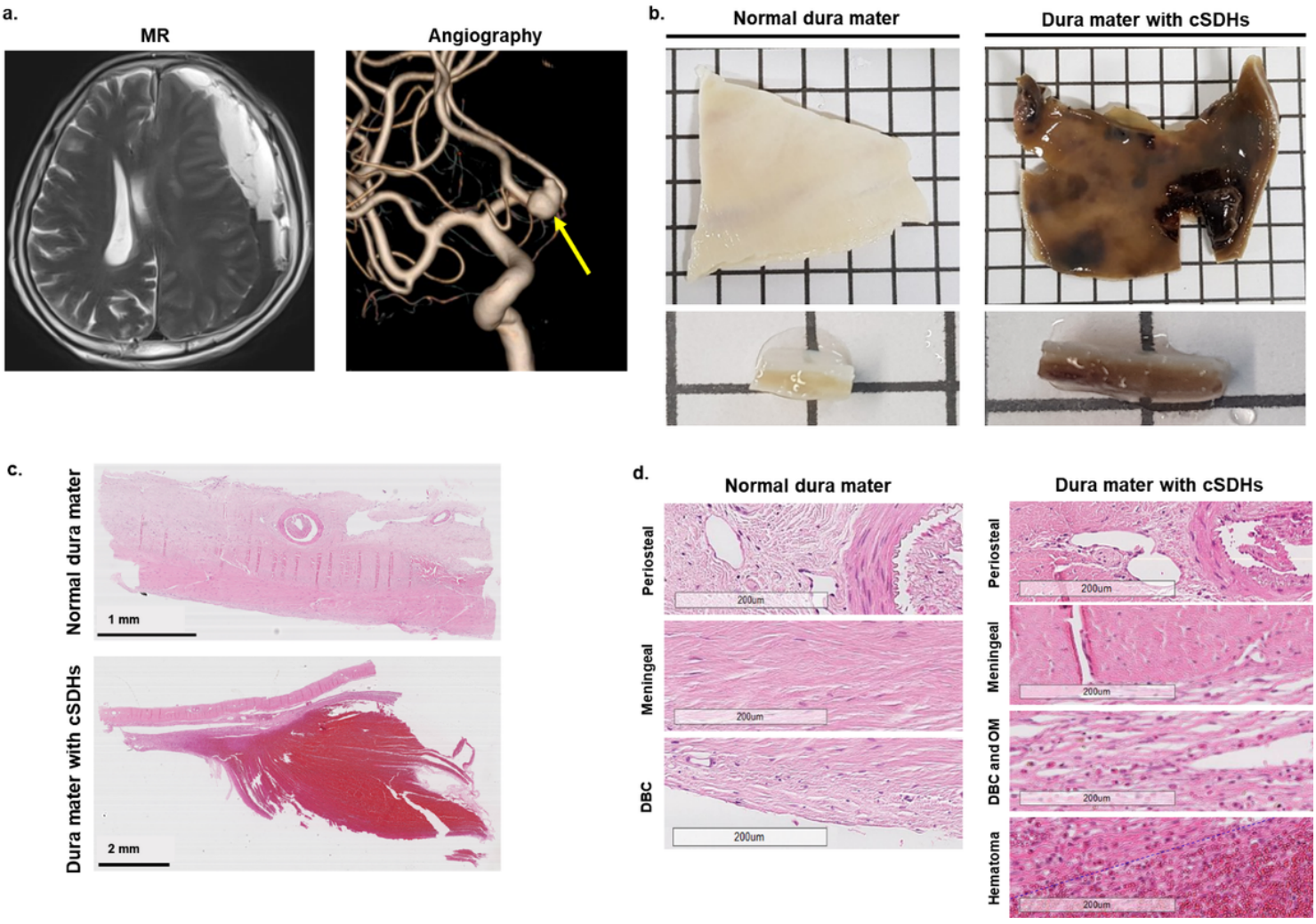

Figure 1

Imaging and histologic data. **(a)**. MR and 3D reconstructive angiographic images of a patient with repeat spontaneous cSDHs. The patient underwent clipping of the unruptured intracranial aneurysm at the anterior communicating artery (yellow arrow, right) and removal of cSDHs with adjacent dura mater and OM (left) simultaneously via left-sided frontotemporal craniotomy. **(b)**. Gross photos of the normal control and pathologic dura mater attached to the OM of cSDHs. **(c, d)**. Representative H&E staining

images of the dura mater from the normal control and patient with cSDHs. Scale bar: 1 mm, normal dura mater; 2 mm, dura mater with cSDHs. d. In the high magnification images, the DBC layer and OM of cSDHs showed looser connective tissue and numerous cavities than the DBC layer in the normal control. The blue line indicates the boundary between the OM and hematoma. Scale bar, 200 μm

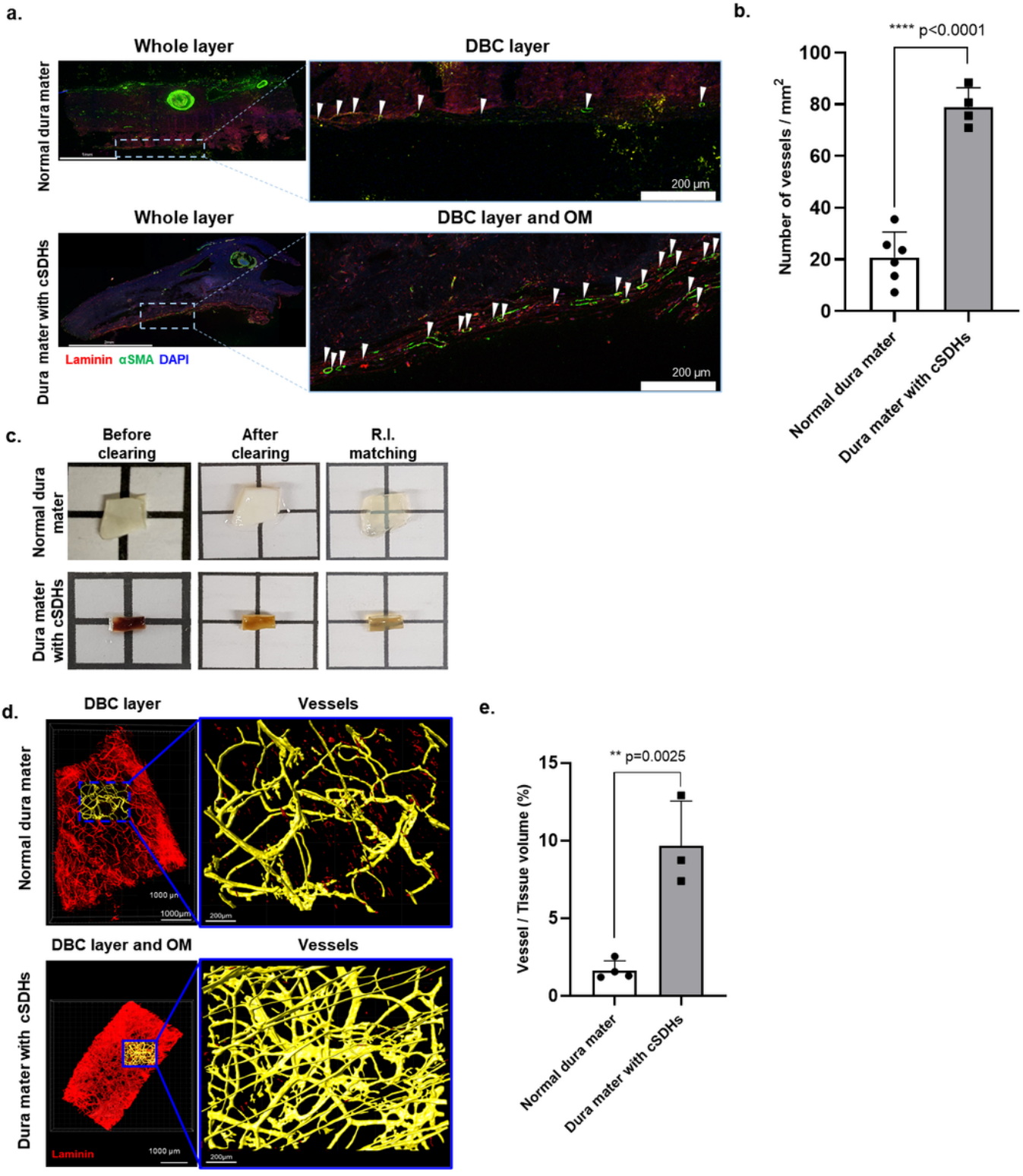

Figure 2

Neovascularization in the DBC layer of the dura mater and OM of cSDHs. (**a)**. Representative images of vessels immunolabeled with laminin (red) and αSMA (green) in the dura mater of the normal control (scale bar, 1 mm) and patient with cSDHs (scale bar, 2 mm). There was a greater increase in vessels in the DBC layer and OM of cSDHs compared to the normal control. White arrowheads indicate vessels. Scale bar, 200 μm. (**b)**. Quantification of the number of vessels per area (mm^2) of the DBC layer. Each dot represents the number of vessels from 4~6 sections in the dura mater. Data are presented as the AVE ± SD (*P < 0.05, **P < 0.005). (**c)**. Schematic of the procedure for preparing transparent tissue samples. After clearing, the images showed the removal of lipids from the polymerized tissue. Refractive index (R.I.)-matched tissues were transparent. (**d).** Representative images of the 3D vasculature stained with laminin in the normal control and DBC layer and OM of cSDHs in the patient. Scale bar, 1 mm. The vessels in the volume-rendered images are shown in yellow at 5X magnification (scale bar, 200 μm). (**e)**. Quantification of the vascular volume per tissue volume ($μm^3$). The total volume of vessels was higher in the specimen from the patient with cSDHs than in that from the normal control. Data are presented as the AVE ± SD (*P < 0.05, **P < 0.005)

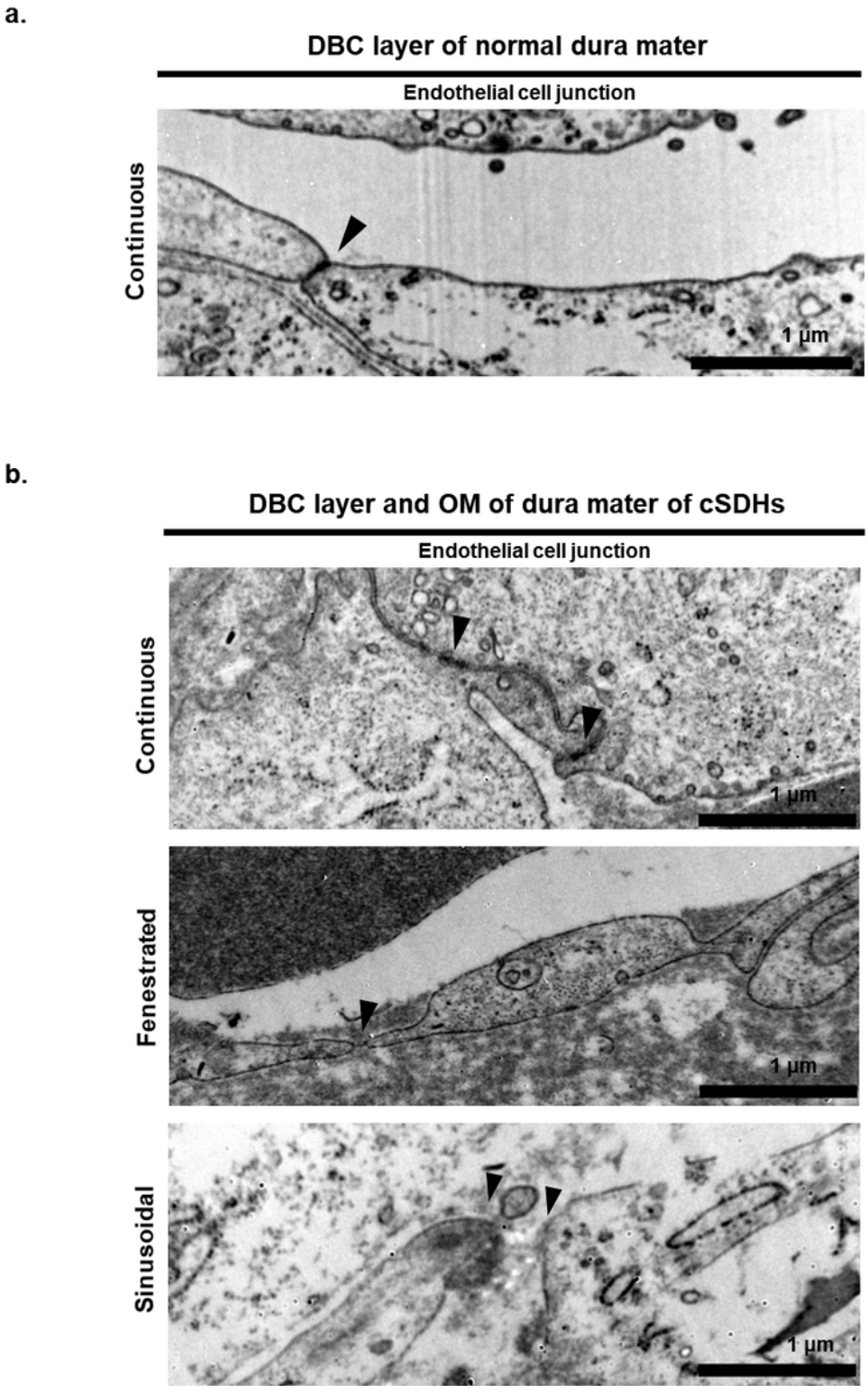

Figure 3

Types of capillaries in the DBC layer of the dura mater and OM of cSDHs. (**a).** Representative TEM image of a continuous capillary in the DBC layer of the normal control. The black arrowhead indicates a tight junction between endothelial cells. Scale bar, 1 μm. (**b).** Representative TEM images of the capillary type in the DBC layer of the dura mater and OM of cSDHs from the patient. Black arrowheads indicate tight

junctions in a continuous capillary, a pore with a diaphragm in a fenestrated capillary, and gaps without junctions and diaphragms in a sinusoidal capillary. Scale bar, 1 μm

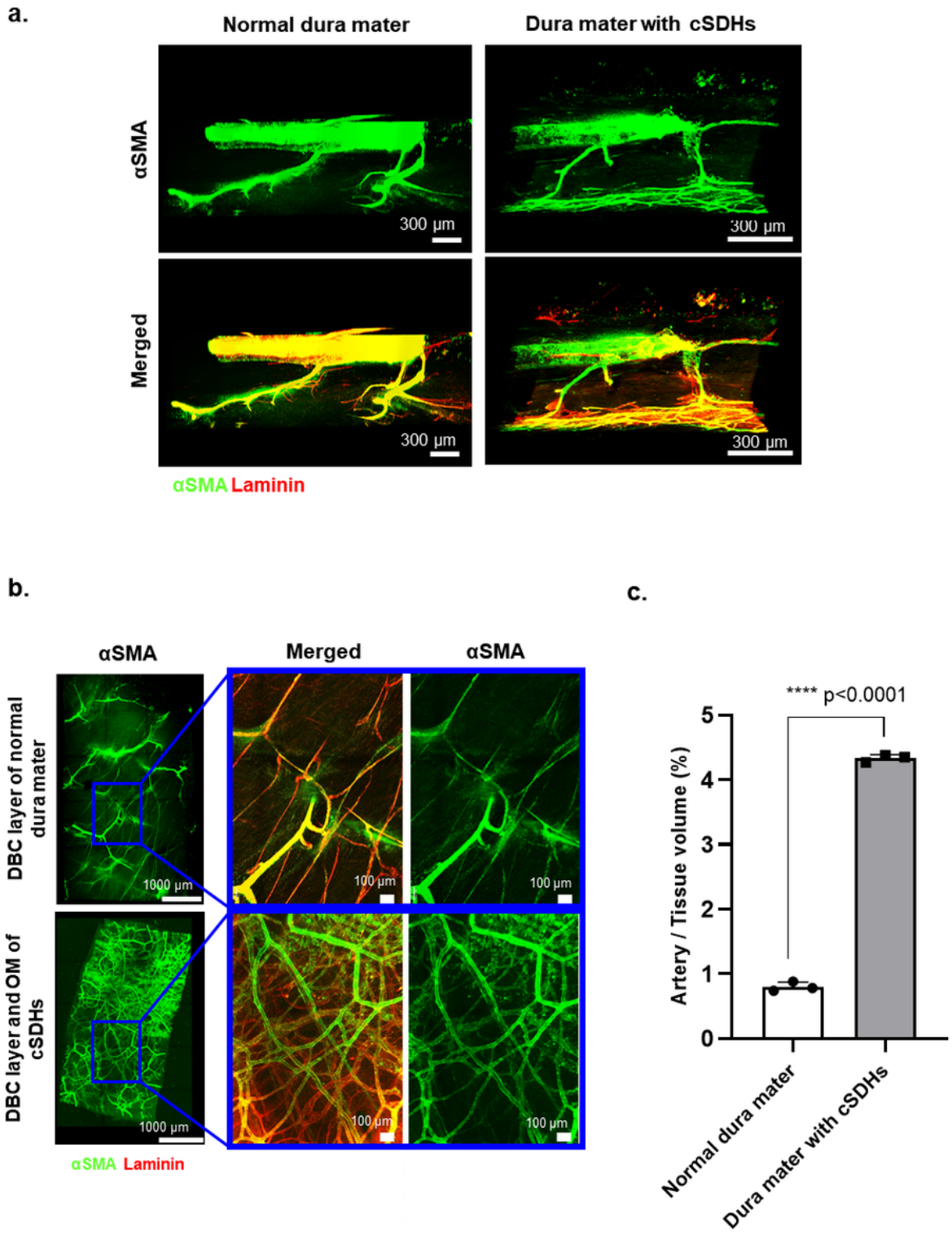

Figure 4

Connection between MMAs and newly formed capillaries in the DBC layer and OM of cSDHs. (**a).** Representative images of 3D vessels stained with laminin (red) and αSMA (green) in the entire dura mater

from the periosteal to the DBC layers. The penetrating arteries connected to the MMAs in the periosteal layer and the capillaries in the DBC layer. A significant increase in capillaries in the DBC layer and OM of cSDHs was observed. Scale bar, 300 μm. **(b)**. Laminin (red)- and αSMA (green)-labeled arteries are shown after volume rendering steps. The 3D volume of the capillaries in the DBC dural layer and OM of cSDHs is shown in yellow. (**c**). Quantification of the arterial volume (μm^3) in the DBC layer and OM. The volume of capillaries increased significantly. Data are presented as the AVE ± SD (*P < 0.05, **P < 0.005)

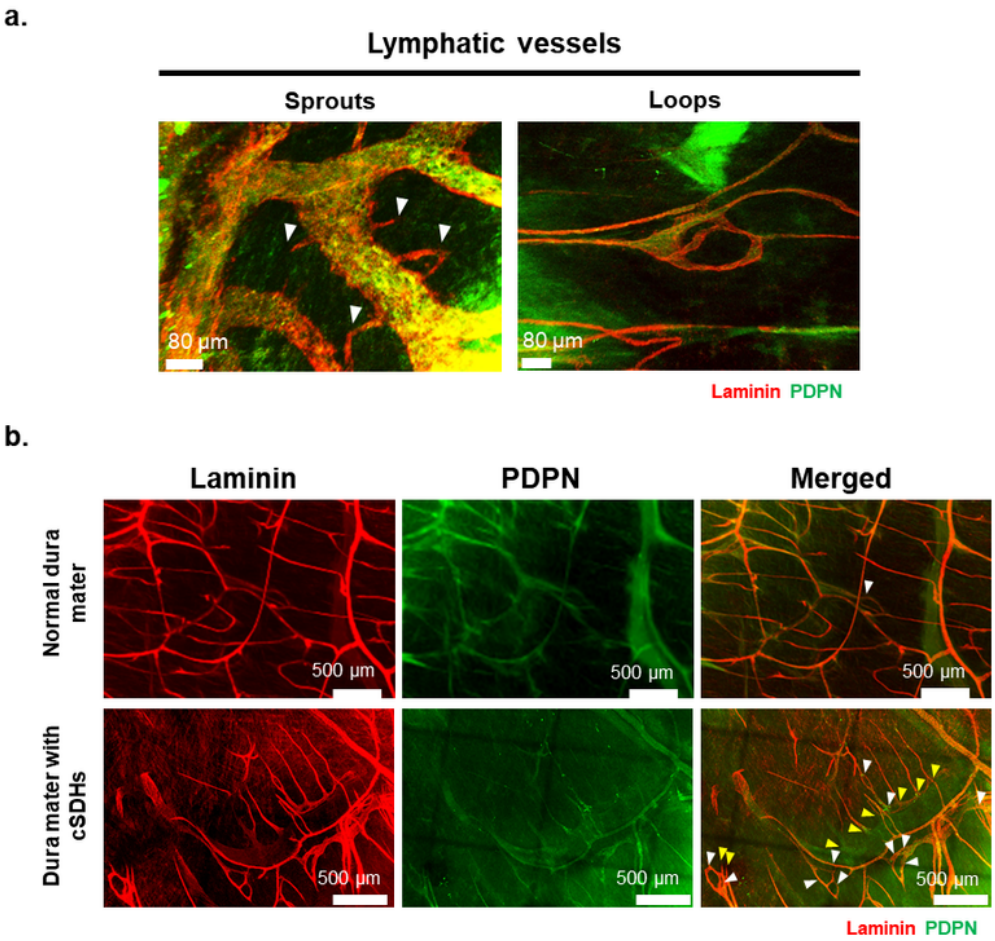

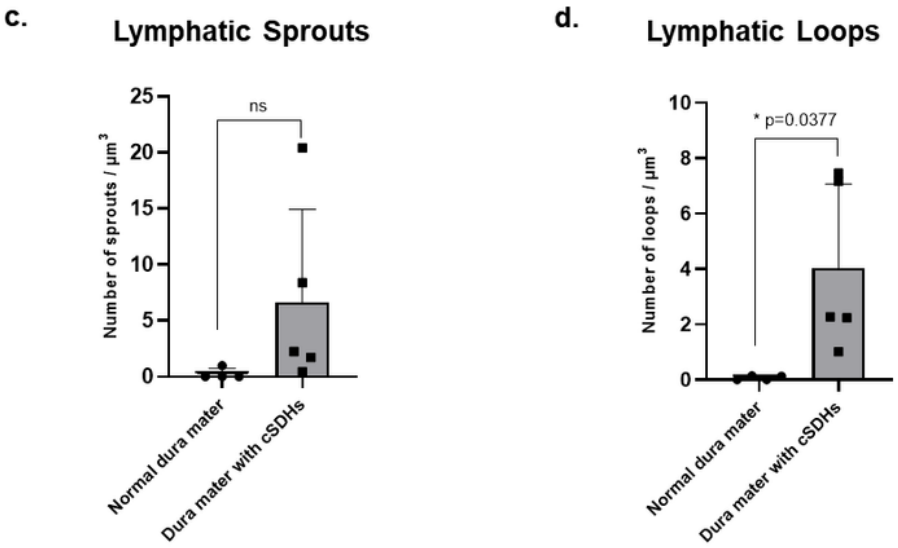

Figure 5

The formation of lymphatic vessels. (**a**). Representative images of immunostaining of vessels (laminin, red) and lymphatic vessels (PDPN, green) in the periosteal and meningeal layers of 4 pieces of tissue. The white and yellow arrowheads indicate the loops and sprouts of lymphatic vessels, respectively. (**b**). Representative magnified images of loops and sprouts in lymphatic vessels. (**c**). Quantification of the number of loops and sprouts per area (μm^3) in the dura mater. Greater formation of loops and sprouts was observed in the patient with cSDHs than in the normal control. Data are presented as the AVE ± SD (*$P < 0.05$).

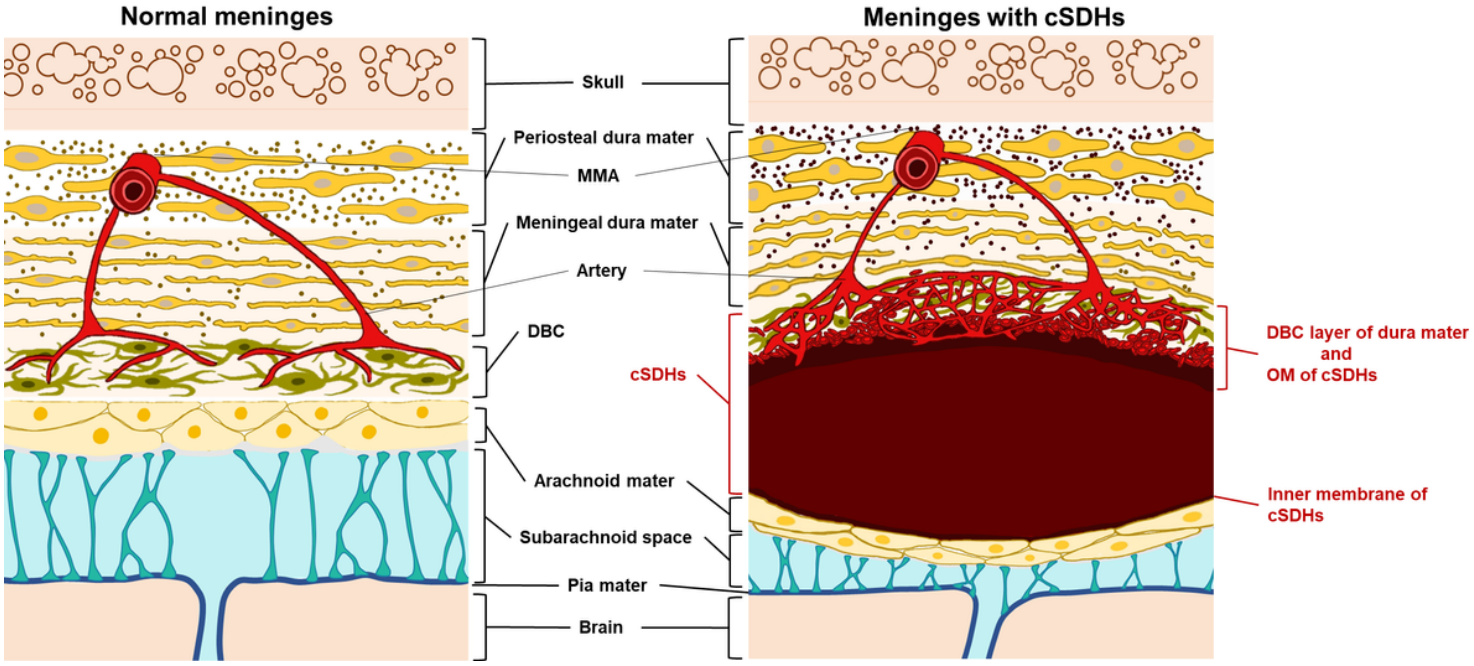

Figure 6

Illustration of the pathological characteristics of the dura mater and cSDHs. As the hematoma accumulates in the subdural space, membranes envelop the cSDHs. Compared to the inner membrane of cSDHs, the OM of cSDHs seems to originate from the DBC layer of the dura mater based on the histologically indistinguishable plane between the DBC layer and OM. The number of vessels in the DBC layer and OM in the patient with cSDHs was much higher than that in the DBC layer of the normal control. Newly formed vessels are composed of sinusoidal capillaries, which are thought to be a probable cause of repeat spontaneous bleeding because they are fragile and present in only the pathological DBC dural layer and OM of cSDHs. Such neovessels connect to surface MMAs via penetrating arteries. Therefore, MMA embolization is a potentially effective way to block the blood supply to pathological membranes.

Supplementary Files

This is a list of supplementary files associated with this preprint. Click to download.

- 20220527SupplementalMaterial.docx
- SupplementaryVideo1.mp4
- SupplementaryVideo2.mp4